

Fusion of ${}^9\text{Li}$ with ${}^{208}\text{Pb}$

A. M. Vinodkumar,^{1,*} W. Loveland,¹ P. H. Sprunger,¹ L. Prisbrey,¹ M. Trinczek,² M. Dombisky,² P. Machule,² J. J. Kolata,³ and A. Roberts³

¹*Department of Chemistry, Oregon State University, Corvallis, Oregon 97331, USA*

²*TRIUMF, Vancouver, British Columbia V6T 2A3, Canada*

³*Department of Physics, University of Notre Dame, Notre Dame, Indiana 46556, USA*

(Received 1 August 2009; published 23 November 2009)

We have measured the fusion excitation function for the ${}^9\text{Li} + {}^{208}\text{Pb}$ reaction for near-barrier projectile center-of-mass energies of 23.9 to 43.0 MeV using the ISAC2 facility at TRIUMF. The α -emitting evaporation residues (${}^{211-214}\text{At}$) were stopped in the ${}^{208}\text{Pb}$ target, and their decay was measured. The isotopic yields at each energy were in good agreement with the predictions of a statistical model code (HIVAP). The measured fusion excitation function shows evidence for substantial sub-barrier fusion enhancement not predicted by current theoretical models. There is a suppression of the above barrier cross sections relative to these model predictions. The implications of this measurement for studying the fusion of ${}^{11}\text{Li}$ with ${}^{208}\text{Pb}$ are discussed.

DOI: [10.1103/PhysRevC.80.054609](https://doi.org/10.1103/PhysRevC.80.054609)

PACS number(s): 25.70.Jj, 25.85.-w, 25.60.Pj

I. INTRODUCTION

One of the most active areas of research with radioactive beams is the study of the fusion of weakly bound nuclei, such as the halo nuclei. The central issue is whether the fusion cross section will be enhanced because of the large nuclear size of the halo nucleus or whether fusion-limiting breakup of the weakly bound valence nucleons will lead to a decreased fusion cross section. Most theoretical calculations have dealt with the ${}^{11}\text{Li} + {}^{208}\text{Pb}$ reaction, with a wide variety of outcomes. Figure 1 (taken from a review article by Signorini [1]) shows the range of predictions for the sub-barrier fusion cross sections, which span four orders of magnitude. It is clear that a measurement of the fusion excitation function for the ${}^{11}\text{Li} + {}^{208}\text{Pb}$ reaction would be valuable in resolving the differences between the various predictions shown in Fig. 1.

The general problem of the near-barrier fusion and breakup reactions of weakly bound nuclei has been studied, with differing conclusions. For the ${}^6\text{He} + {}^{209}\text{Bi}$ reaction [2,3], enhanced sub-barrier fusion was observed, whereas in the ${}^6\text{He} + {}^{238}\text{U}$ reaction [4], a possible suppression of sub-barrier fusion was observed. For the ${}^9\text{Be} + {}^{208}\text{Pb}$ reaction [5], ${}^9\text{Be} + {}^{209}\text{Bi}$ reaction [6], ${}^{6,7}\text{Li} + {}^{209}\text{Bi}$ reactions [5], and ${}^6\text{Li} + {}^{208}\text{Pb}$ reaction [7], a large suppression of fusion above the barrier has been observed. For the ${}^{11}\text{Be} + {}^{209}\text{Bi}$ [8,9] and the ${}^{19}\text{F} + {}^{208}\text{Pb}$ systems [10], the effect of breakup on the fusion cross section was negligible.

Our group has been engaged in a deliberate careful approach to measuring the ${}^{11}\text{Li} + {}^{208}\text{Pb}$ fusion excitation function. We started by studying the fusion of ${}^9\text{Li}$ with ${}^{70}\text{Zn}$ using the ISAC facility at TRIUMF. ${}^{70}\text{Zn}$ was chosen as the target nucleus because the “energy limit” (at that time) of the ISAC beams of 1.7 A MeV prevented one from reaching the fusion barrier in heavier systems. The results of this study [11] showed a large sub-barrier fusion enhancement for the reaction of ${}^9\text{Li}$ with ${}^{70}\text{Zn}$ that was not accounted for

by current models of fusion (Fig. 2). Attempts to describe these results [12,13] required unusual mechanisms to enhance sub-barrier fusion in these systems. Zagrebaev *et al.* [12] found that standard coupled-channel calculations along with neutron transfer were not able to describe the observed sub-barrier fusion and postulated “dineutron transfer” to account for the observed data. Balantekin and Kocak [13] also found that coupled-channel calculations including inelastic excitation and one-neutron transfer failed to reproduce the data and suggested the possible formation of a molecular bond accompanied by two-neutron transfer to account for the observed behavior. In this approach, the neutron-rich ${}^{70}\text{Zn}$ contributes two neutrons to form the ${}^{11}\text{Li}$ halo structure in the nuclei at contact, which enhances the fusion cross section. The data [11] are well represented by this model.

We believe these observations are significant because ${}^9\text{Li}$ is the “core” of the two-neutron halo nucleus ${}^{11}\text{Li}$. Many calculations have suggested that in the interaction of ${}^{11}\text{Li}$ with ${}^{208}\text{Pb}$, the ${}^{11}\text{Li}$ will break up into two neutrons and the ${}^9\text{Li}$ core, which in turn will fuse with the ${}^{208}\text{Pb}$ nucleus. In the study of Petrascu [14] of the fusion of ${}^{9,11}\text{Li}$ with Si at 11.2–15.2 A MeV, the author found evidence that the ${}^9\text{Li}$ fused with the Si, but in the case of ${}^{11}\text{Li}$, there was emission of one or two neutrons prior to fusion. Thus, we felt that a study of the fusion of ${}^9\text{Li}$ with ${}^{208}\text{Pb}$ would be an important step toward understanding the fusion of ${}^{11}\text{Li}$ with ${}^{208}\text{Pb}$.

The reaction of ${}^9\text{Li}$ with ${}^{208}\text{Pb}$ has been studied theoretically by Takigawa *et al.* [15]. They simply assumed the validity of the Wong formula [16] and calculated the fusion excitation function. These results are compared with our measurements in the following discussion.

In Sec. II, we describe the experimental arrangements, whereas in Sec. III, we describe and discuss the results of the measurement.

II. EXPERIMENTAL

A. Setup and design

The measurement of the fusion cross section for the ${}^9\text{Li} + {}^{208}\text{Pb}$ reaction was carried out at the ISAC2 facility

*Present address: Department of Physics, University of Calicut, Kerala 673635, India.

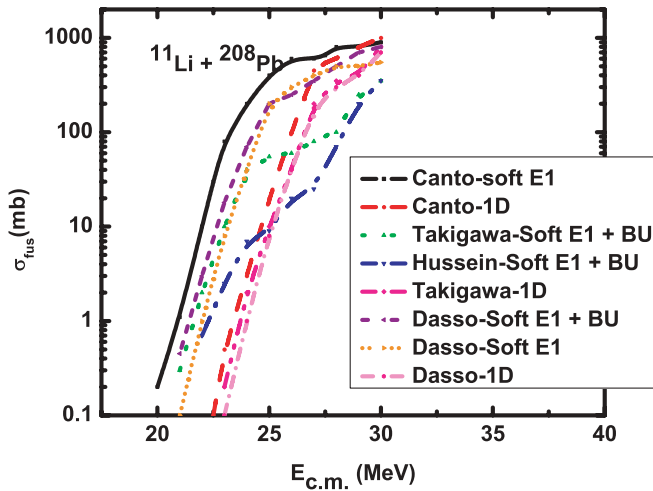


FIG. 1. (Color online) Various theoretical predictions for the sub-barrier fusion cross sections for the $^{11}\text{Li} + ^{208}\text{Pb}$ reaction. From Ref. [1]. See Ref. [1] for the details of the various predictions.

at TRIUMF. Proton beams (500 MeV) with an intensity of $\sim 70 \mu\text{A}$ struck Ta metal production targets. Beams of radioactive ^9Li were extracted with energies up to 18.4 keV, mass-separated by passage through two dipole magnets, and accelerated to their final energy by radiofrequency quadrupole and drift-tube linear accelerators. The details of the production of these secondary beams are discussed elsewhere [17,18]. The stable ^7Li beam used to calibrate the efficiency of the experimental setup (as will be discussed) was generated using a local ion source.

The experiment was set up on the straight-through beam line of the ISAC2 facility. The experiment was carried out in a large (~ 35 L), thin-walled spherical scattering chamber mounted on this beam line. The ^9Li (^7Li) beams struck ^{208}Pb (^{209}Bi) targets mounted at the center of the chamber. Beam intensities were monitored by detecting elastic scattering at $\pm 16^\circ$ with additional monitoring of the beam by a suppressed

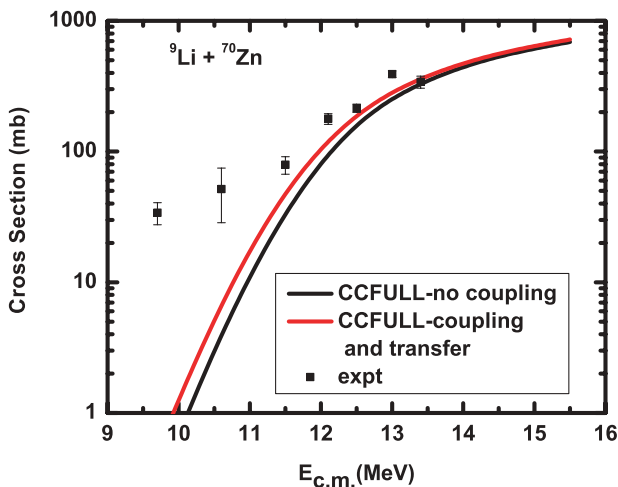


FIG. 2. (Color online) Comparison of the fusion excitation function for the $^9\text{Li} + ^{70}\text{Zn}$ reaction with coupled-channel calculations [11].

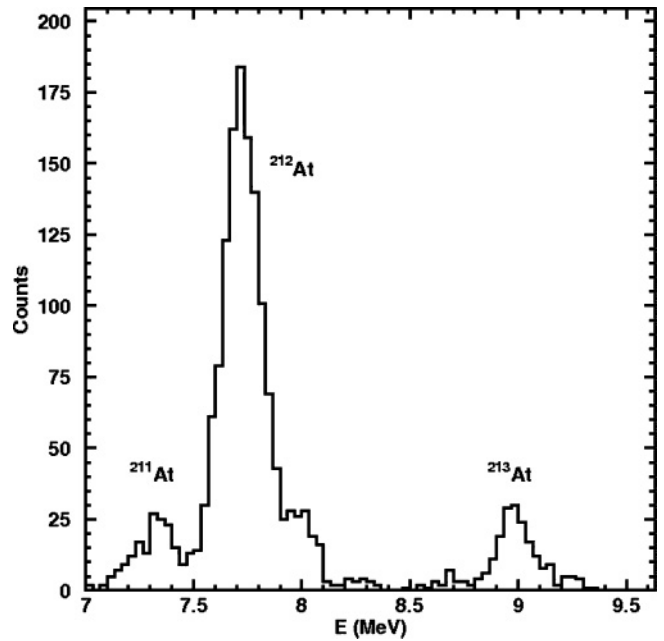


FIG. 3. A typical α -particle spectrum from the interaction of 45-MeV ^9Li with ^{208}Pb .

Faraday cup at the end of the beam line. (A 0.008-m^3 5% boron-loaded paraffin shield was used to reduce the neutron emission from the Faraday cup to acceptable levels ($1 \mu\text{Sv/h}$ at 3 m). ^9Li is a 178-ms β emitter with a $Q_\beta \sim 13.6$ MeV with $\sim 50\%$ of the decays resulting in neutron emission. The average on-target ^9Li intensity was $10^7/\text{s}$, and the average on-target ^7Li intensity was $2.5 \times 10^9/\text{s}$. Both beams were pulsed with the beam being on for 172 ns and then off for 172 ns. The ^{208}Pb target was 0.903 mg/cm^2 thick, and the ^{209}Bi target was 0.465 mg/cm^2 thick.

An array of 18 (300 mm^2) Si detectors surrounding the target was used to detect decay α -particles emitted from evaporation residues (EVRs) that stopped in the Pb/Bi targets in the beam-off period. The geometrical efficiency of the array for detecting decay α particles emitted by the EVRs that stopped in the targets was evaluated by a Monte Carlo simulation to be 20%. A typical α spectrum is shown in Fig. 3.

EVR cross sections were measured for the interaction of 24.8, 27.4, 29.9, 32.4, 34.9, 37.4, 39.9, 42.4, and 44.9 MeV ^9Li with ^{208}Pb . (These energies represent center-of-target energies, calculated from the incident beam energies and the energy loss of the projectiles in a target half-thickness [19].) Typical doses were $\sim 0.3 \times 10^{12}$ particles at each energy. In the calibration reaction involving the $^7\text{Li} + ^{209}\text{Bi}$ reaction, the ^7Li center-of-target beam energy was 34.95 MeV.

B. α -decay measurements

The α -emitting EVRs produced in the $^9\text{Li} + ^{208}\text{Pb}$ reaction are astatine isotopes, specifically $^{211-214}\text{At}$. In Table I, we summarize the decay properties of these nuclei. These activities are produced and decay during irradiation in accord with the equations of radioactive decay. All decays of the metastable states to lower lying states by isomeric transition (IT) decay

TABLE I. Decay properties of the astatine EVRs observed in this work.

Isotope	$t_{1/2}$ (s)	E_α (keV) (% abundance)
${}^{211}\text{At}$	25,970	5869.5(41.8)
${}^{212}\text{At}$	0.314	7679(82); 7616(16)
${}^{212}\text{At}^m$	0.119	7837(66); 7900(31.5)
${}^{213}\text{At}$	125×10^{-9}	9080(100)
${}^{214}\text{At}$	558×10^{-9}	8819(98.95)
${}^{214}\text{At}^{m1}$	265×10^{-9}	8877(100)
${}^{214}\text{At}^{m2}$	760×10^{-9}	8782(99.18)

are negligible. For nuclei that are produced directly during the irradiation, the number of atoms present, N_2 , after a “beam-on” period of t seconds is given as

$$N_2(t) = N_2(0) \exp(-\lambda_2 t) + \frac{R_2}{\lambda_2} [1 - \exp(-\lambda_2 t)], \quad (1)$$

where $N_2(0)$ is the number of nuclei present at the beginning of the period, R_2 is the rate of production ($\equiv N_{\text{target}} \sigma \phi$), λ_2 is the decay constant, N_{target} is the number of target atoms, σ is the cross section, and ϕ is the beam intensity. During the “beam-off” period, the number of atoms decreases because of decay

$$N_2(t) = N_2(0) \exp(-\lambda_2 t). \quad (2)$$

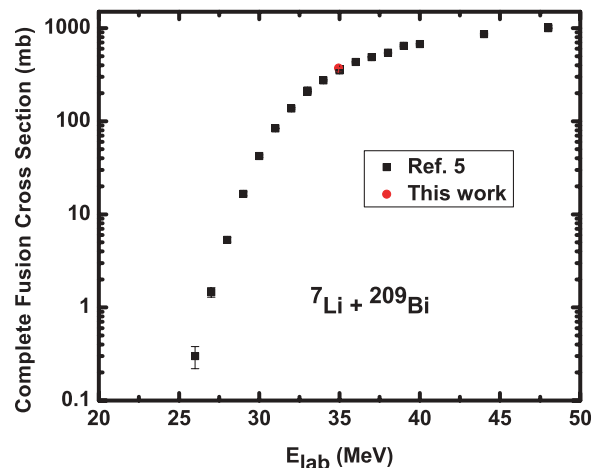
It is straightforward to show that when the total “beam-on” time is long compared with the half-lives of the nuclide involved, the number of decays of product atoms per “beam off” period is a constant fraction of the term $\frac{R_2}{\lambda_2}$. For the long-lived ${}^{211}\text{At}$, its decay was measured via its 58.2% electron capture (EC) branch to α -emitting ${}^{211}\text{Po}$. Standard equations of production and decay were used to describe this decay, which was detected after the end of each irradiation.

C. Efficiency calibration

To check that we understood all aspects of the measurement of nuclidic activities, we also measured the yield of the evaporation residues ${}^{212,213}\text{Rn}$ formed in the reaction of 34.95-MeV ${}^7\text{Li}$ with ${}^{209}\text{Bi}$ and compared our results with the previous measurement of Dasgupta *et al.* [5]. Our results are shown in Table II and Fig. 4. The agreement is excellent, indicating we can reproduce known information about similar reactions.

TABLE II. Comparison of our EVR measurements for the ${}^7\text{Li} + {}^{209}\text{Bi}$ reaction with Ref. [5].

Isotope	Cross section (mb) [5]	Cross section (mb)—this work
${}^{213}\text{Rn}$	195.0 ± 3.2	208.8 ± 1.4
${}^{212}\text{Rn}$	154.3 ± 4.9	158.9 ± 1.2
Fission	3.16 ± 0.03	Not measured
Complete fusion cross section	352.5 ± 5.9	370.9 ± 1.8

FIG. 4. (Color online) Comparison of EVR measurements for the ${}^7\text{Li} + {}^{209}\text{Bi}$ reaction.

III. RESULTS AND DISCUSSION

A. Cross sections

The nuclidic production cross sections for the ${}^9\text{Li} + {}^{208}\text{Pb}$ reaction are given in Table III and shown in Fig. 5, along with predictions of the statistical model code HIVAP [20] for this reaction. The input parameters and other choices in running HIVAP were taken from the “Reisdorf-Schädel” standard parameter set [21]. The agreement between the predicted and measured values of the production cross sections is excellent, spanning an order of magnitude. No other fusion-like products were observed, and HIVAP does not predict the formation of other fusion-like products other than the observed astatine nuclei.

The observed fusion cross sections are given in Table III and are shown in Fig. 6. In computing these cross sections, we have ignored any cross section associated with fusion-fission as we expect that component of the fusion cross section to be small [5]. In Fig. 6, we compare the measured values of the fusion cross sections with the previously mentioned

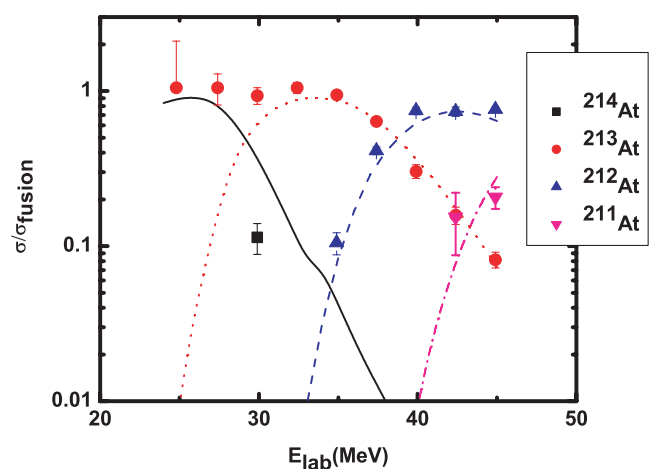
FIG. 5. (Color online) Comparison of measured nuclidic yields (data points) from the ${}^9\text{Li} + {}^{208}\text{Pb}$ reaction with predictions of the HIVAP statistical model code (lines).

TABLE III. Measured nuclidic cross sections for the ${}^9\text{Li} + {}^{208}\text{Pb}$ reaction.

Beam energy (cot-MeV)	${}^{214}\text{At}$ (mb)	${}^{213}\text{At}$ (mb)	${}^{212}\text{At}$ (mb)	${}^{211}\text{At}$ (mb)	Total cross section (mb)
24.84	–	0.61 ± 0.61	–	–	0.61 ± 0.61
27.35	–	8.4 ± 1.9	–	–	8.4 ± 1.9
29.86	8.4 ± 1.9	69.3 ± 8.4	–	–	77.7 ± 8.6
32.36	–	287 ± 23	–	–	287 ± 23
34.87	–	403 ± 17	45 ± 7.3	–	448 ± 19
37.37	–	400 ± 18.9	259 ± 14.7	–	659 ± 24
39.88	–	218 ± 22	534 ± 29	–	752 ± 37
42.38	–	133 ± 17	620 ± 43	129 ± 56	882 ± 73
44.89	–	72 ± 8.4	669 ± 23	182 ± 29	923 ± 39

predictions of Takigawa *et al.* [15]. Compared with these predictions, the measured fusion excitation function shows evidence of enhanced sub-barrier fusion and suppression of fusion above the barrier.

B. Comparison with previous measurements

In Fig. 7, we show the measured fusion excitation functions for the ${}^6\text{Li} + {}^{208}\text{Pb}$ [7], ${}^7\text{Li} + {}^{208}\text{Pb}$ [5], ${}^8\text{Li} + {}^{208}\text{Pb}$ [22], and the ${}^9\text{Li} + {}^{208}\text{Pb}$ (this work) reactions. What is presented in Fig. 7 are the “reduced” excitation functions in which each fusion cross section is divided by πR_B^2 and each energy is shown as $E_{c.m.}/V_B$, where R_B and V_B are the fusion radii and barrier heights in the semiempirical Bass model [23]. All the “reduced” excitation functions appear to be similar. This would indicate the basic differences between these different Li nuclei in their interaction with ${}^{208}\text{Pb}$ are geometrical in origin.

C. Comparison with theory

There are two possible breakup/transfer channels in the ${}^9\text{Li} + {}^{208}\text{Pb}$ reaction that deserve further scrutiny. They are the ${}^9\text{Li} + {}^{208}\text{Pb} \rightarrow {}^7\text{Li} + {}^{210}\text{Pb}$ reaction ($Q = +3.0$ MeV) and

the ${}^9\text{Li} + {}^{208}\text{Pb} \rightarrow {}^8\text{Li} + {}^{209}\text{Pb}$ reaction ($Q = -0.1$ MeV). The heavy products of these reactions, ${}^{209}\text{Pb}$ and ${}^{210}\text{Pb}$, could not be detected in our experiment because of their decay mode (β^- decay) and relatively long half-lives. Given the positive or near-zero Q values for these reactions, one might expect them to contribute uniformly over the energy range studied to the total reaction cross section. Because they are not fusion-like events, they do not contribute to the total fusion cross section, but they can be a contributor to the overall “suppression” of fusion above the barrier.

Another possibility to be considered is the breakup of ${}^9\text{Li}$ into two charged fragments, which in turn may individually fuse with ${}^{208}\text{Pb}$ to form observable EVRs. The most likely process of this type is the breakup of ${}^9\text{Li}$ into ${}^4\text{H}$ and ${}^5\text{He}$ ($Q = -2.4$ MeV). (Other possible breakup/incomplete fusion processes have much larger negative Q values.) In this case, the fusion of the ${}^5\text{He}$ fragment with ${}^{208}\text{Pb}$ is expected to have a negligible cross section based on calculations with the statistical model code HIVAP [20]. However, the ${}^4\text{H}$ fragment should have a substantial probability (HIVAP) to fuse with ${}^{208}\text{Pb}$ producing the completely fused system ${}^{212}\text{Bi}$. According to simulations of this reaction using the HIVAP code, 97% of

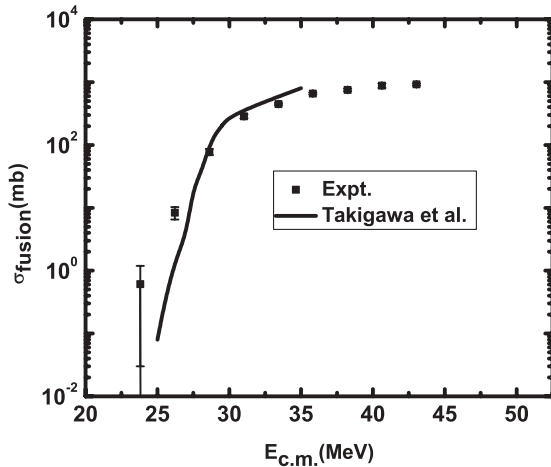


FIG. 6. Comparison of measured fusion cross sections (data points) from the ${}^9\text{Li} + {}^{208}\text{Pb}$ reaction with Ref. [15] (lines).

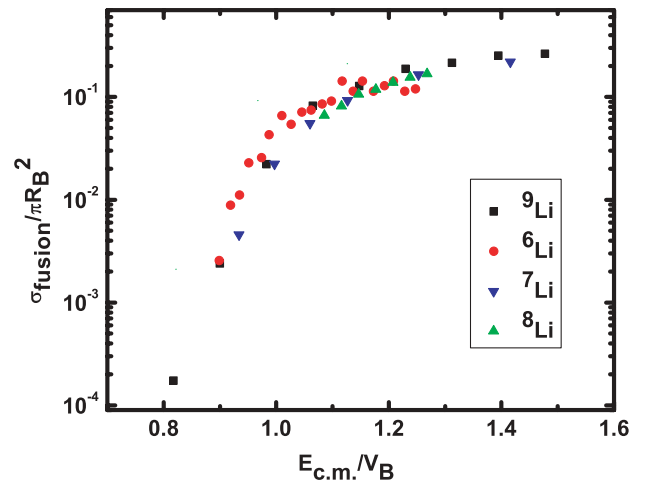


FIG. 7. (Color online) Comparison of the “reduced” fusion excitation functions for the ${}^6\text{Li} + {}^{208}\text{Pb}$ [7], ${}^7\text{Li} + {}^{208}\text{Pb}$ [5], ${}^8\text{Li} + {}^{208}\text{Pb}$ [22], and ${}^9\text{Li} + {}^{208}\text{Pb}$ (this work) reactions.

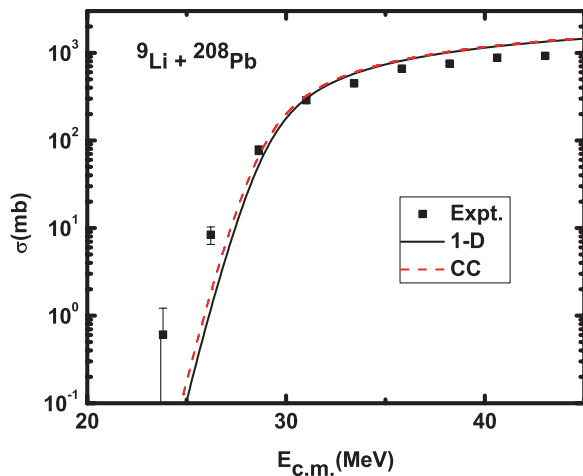


FIG. 8. (Color online) Comparison of the measured fusion excitation function for the ${}^9\text{Li} + {}^{208}\text{Pb}$ reaction with the predictions of coupled-channel calculations.

the ${}^{212}\text{Bi}$ nuclei formed in this manner de-excite, by neutron emission, to form stable ${}^{209}\text{Bi}$, a nuclide that is not detectable in this experiment. Thus, this breakup process cannot contribute to the observed fusion cross sections although the occurrence of this reaction above the barrier can contribute to a repression of the fusion cross section relative to the total reaction cross section.

D. Coupled-channel calculations

It is traditional to compare the sub-barrier fusion cross sections in works such as ours with the predictions of coupled-channel calculations. We have used the code CCFULL [24] to make this comparison. We assumed a potential $V_0 = 105$ MeV, $r_0 = 1.12$ fm, and diffuseness parameter $a = 0.65$ fm. We included the inelastic excitation of the rotational states in ${}^9\text{Li}$ [25] and the first vibrational 3^- state in ${}^{208}\text{Pb}$ at 2.615 MeV, $B(E3; 0^+ \rightarrow 3^-) = 0.611 e^2\text{b}^3$ [26]. We also included a simple one-dimensional barrier penetration calculation with no coupled-channel effects. In Fig. 8, we compare the results of this calculation with the measured data. The coupled-channel calculations underestimate the sub-barrier fusion cross sections and overestimate the above barrier cross sections.

IV. CONCLUSION

What have we learned from this study?

- (i) We have measured the yields of the astatine EVRs from the ${}^9\text{Li} + {}^{208}\text{Pb}$ reaction. We do not observe other possible fusion-like products from this reaction. From these At yields, we have estimated the total fusion cross sections for this reaction. (In doing so, we have neglected fusion-fission reactions [5] and incomplete fusion reactions that lead to unobservable EVRs.)
- (ii) The measured fusion cross sections, when compared with theoretical predictions [15] or coupled-channel calculations, show enhanced sub-barrier fusion and a suppression of fusion above the barrier. This latter suppression may be caused, in part, by the occurrence of breakup/transfer reactions that cannot be observed in this study and are part of the “fusion” cross section in coupled-channel calculations.
- (iii) The relative yields of the At radionuclides are well described, at each energy studied, by the statistical model code HIVAP.
- (iv) The “reduced” fusion excitation functions for the interaction of ${}^6\text{Li}$, ${}^7\text{Li}$, ${}^8\text{Li}$, and ${}^9\text{Li}$ with ${}^{208}\text{Pb}$ are generally similar, leading one to the conclusion that the primary effects governing the differences in fusion with these projectiles with ${}^{208}\text{Pb}$ are geometrical in origin.
- (v) Because ${}^9\text{Li}$ is the “core” of ${}^{11}\text{Li}$, the results of this study may be useful in characterizing breakup/fusion in the ${}^{11}\text{Li} + {}^{208}\text{Pb}$ reaction.

ACKNOWLEDGMENTS

We thank the operations staff of the cyclotron and at ISAC as well as Marco Marchetti and Robert Laxdal for providing the ${}^9\text{Li}$ beams. We want to thank E. F. Aguilera *et al.* for allowing us to see their data on the ${}^8\text{Li} + {}^{208}\text{Pb}$ reaction prior to publication. This work was supported, in part, by the Office of High Energy and Nuclear Physics, Nuclear Physics Division, US Department of Energy, under Grant No. DE-FG06-97ER41026, and by TRIUMF and the Natural Sciences and Engineering Research Council of Canada and the US National Science Foundation under Grant No. PHY06-52591.

[1] C. Signorini, J. Phys. G: Nucl. Part. Phys **23**, 1235 (1997).
 [2] P. A. DeYoung *et al.*, Phys. Rev. C **58**, 3442 (1998).
 [3] J. J. Kolata *et al.*, Phys. Rev. Lett. **81**, 4580 (1998).
 [4] M. Trotta *et al.*, Phys. Rev. Lett. **84**, 2342 (2000).
 [5] M. Dasgupta *et al.*, Phys. Rev. C **70**, 024606 (2004).
 [6] C. Signorini *et al.*, Eur. Phys. J. A **5**, 7 (1999).
 [7] Y. W. Wu, Z. H. Liu, C. J. Lin, H. Q. Zhang, M. Ruan, F. Yang, Z. C. Li, M. Trotta, and K. Hagino, Phys. Rev. C **68**, 044605 (2003).
 [8] A. Yoshida *et al.*, Phys. Lett. **B389**, 457 (1996).
 [9] C. Signorini *et al.*, Eur. Phys. J. A **2**, 227 (1998).

[10] K. E. Rehm *et al.*, Phys. Rev. Lett. **81**, 3341 (1998).
 [11] W. Loveland *et al.*, Phys. Rev. C **74**, 064609 (2006).
 [12] V. I. Zagrebaev, V. V. Samarin, and W. Greiner, Phys. Rev. C **75**, 035809 (2007).
 [13] A. B. Balantekin and G. Kocak, AIP Conf. Proc. **1072**, 289 (2008).
 [14] M. Petruscu, Phys. Lett. **B405**, 224 (1997).
 [15] N. Takigawa, M. Kuratani, and H. Sagawa, Phys. Rev. C **47**, R2470 (1993).
 [16] C. Y. Wong, Phys. Rev. Lett. **31**, 766 (1973).
 [17] P. Bricault, M. Dombbsky, A. Dowling, and M. Lane, Nucl. Instrum. Methods Phys. Res. B **204**, 319 (2003).

- [18] M. Dombisky, P. Bricault, and V. Hanemaayer, *Nucl. Phys.* **A746**, 32c (2004).
- [19] SRIM 2008 (<http://www.srim.org>).
- [20] W. Reisdorf, *Z. Phys. A* **300**, 227 (1981).
- [21] W. Reisdorf and M. Schädel, *Z. Phys. A* **343**, 47 (1992).
- [22] E. F. Aguilera *et al.*, *Phys. Rev. C* **80**, 044605 (2009).
- [23] R. Bass, *Nuclear Reactions with Heavy Ions* (Springer, New York, 1980).
- [24] K. Hagino, N. Rowley, and A. T. Kruppa, *Comput. Phys. Commun.* **123**, 143 (1999).
- [25] The energy levels for the nuclei in question were taken from the ENSDF files at the National Nuclear Data Center (<http://www.nndc.bnl.gov>), whereas the deformations were taken from S. Raman, C. W. Nestor, and P. Tikkanen, *At. Data Nucl. Data Tables* **78**, 1 (2001).
- [26] R. H. Spear, *At. Data Nucl. Data Tables* **42**, 55 (1989).